References

COCHRAN, W. (1955). *Acta Cryst.* **8**, 473-478.
GIACOVAZZO, C. (1974). *Acta Cryst.* A**30**, 626-630.
GIACOVAZZO, C. (1980). *Direct Methods in Crystallography.* London: Academic Press.
HAUPTMAN, H. (1971). *Z. Kristallogr.* **134**, 28-43.
KARLE, J. (1972). *Acta Cryst.* B**28**, 3362-3369.
KARLE, J. & GILARDI, R. D. (1973). *Acta Cryst.* A**29**, 401-407.
KARLE, J. & KARLE, I. L. (1966). *Acta Cryst.* **21**, 849-859.
NAYA, S., NITTA, I. & ODA, T. (1965). *Acta Cryst.* **19**, 734-747.
PESCHAR, R. & SCHENK, H. (1986). *Acta Cryst.* A**42**, 309-317.
SHMUELI, U., RABINOVICH, S. & WEISS, G. H. (1989). *Acta Cryst.* A**45**, 361-367.
SHMUELI, U. & WEISS, G. H. (1985). *Acta Cryst.* A**41**, 401-408.
SHMUELI, U. & WEISS, G. H. (1986). *Acta Cryst.* A**42**, 240-246.
SHMUELI, U., WEISS, G. H., KIEFER, J. E. & WILSON, A. J. C. (1984). *Acta Cryst.* A**40**, 651-660.

Acta Cryst. (1989). A**45**, 371-380

Comparison Between Gaussian and Exponential Charge Distributions in Ewald Surface Potentials and Fields: NaCl, Aragonite, Phlogopite

BY C. S. STROM AND P. HARTMAN

Institute of Earth Sciences, State University of Utrecht, PO Box 80021, 3508 *TA Utrecht, The Netherlands*

(*Received* 29 *September* 1987; *accepted* 3 *January* 1989)

Abstract

A comparative study has been undertaken of the employment of Gaussian and exponential charge distribution functions in calculating Coulomb potentials, energies and fields at arbitrary points due to lattice slices, using the Ewald method. The APL program *SURFPOT* has been developed for this purpose, for a general crystal structure with user-defined slice orientations and slice boundary configurations. Results are presented for the (111) face of NaCl, (001) and (112) faces of aragonite ($CaCO_3$) and (001) face of phlogopite ($KM_3T_4O_{10}(OH)_2$, M = divalent cation, $T_4 = Si_3Al$]. The convergence behaviour of the potential sums is consistently and considerably better when the Gaussian form is used.

1. Introduction

Since the predominant mechanism of crystal growth is growth by slices, the availability of generally applicable methods for calculating potentials, electric fields, energies and interaction energies of lamina-shaped lattices is essential to the study of crystal growth. The slices under consideration are parallel to (*hkl*), have infinite extent in two dimensions and thickness d_{hkl}, or some fraction thereof, in the third. They are charge-neutral and usually nonpolar. The points at which potentials and fields are required are arbitrary and may be outside the slice or within it or coinciding with ion sites. Formulating the problem for the face (001) instead of (*hkl*) does not constitute any real limitation. A new unit cell can always be found, such that the required face (*hkl*) in terms of the original cell parameters becomes transformed to (001) in terms of the new.

The most widespread method for calculating Coulomb potentials in ionogenic structures is the method of Ewald (1921). It is essentially based on the introduction of a continuous spherically symmetric charge distribution function σ dependent on an adjustable parameter η, in addition to the distance from a given ion (Tosi, 1964). Thus the charge density, and hence also the potential, are split into two contributions; one formulated in the direct lattice, the other in the reciprocal. Each potential sum converges independently but depends on η, whereas the total potential is independent of η. Thus η functions as the radius of a convergence sphere and is adjusted so as to optimize the convergence of both sums. As will be shown in § 2, neutrality of the unit cell guarantees convergence of the potential expression for an individual slice.

The Ewald method assumes its simplest form in the case of an infinite lattice but has been extended to laminas and to semi-infinite lattices, which are infinite only on one side of a plane, the other side being empty (Hartman, 1958; Heyes & van Swol, 1981). The lamina case is most useful because the laminas may be stacked at will. Should an infinite or semi-infinite lattice be of interest, then a limited number of slices need to be stacked to obtain the most satisfactory approximation, *i.e.* convergence in the third dimension, provided the chosen unit cell possesses no component of dipole moment perpendicular to (*hkl*).

The traditionally chosen functional dependence of σ on the distance from a given ion is Gaussian, but several other possibilities, including the exponential, have been proposed and applied, mostly to rather simple structures. Such an application to a cubic

0108-7673/89/060371-10$03.00

structure with two ions led Heyes (1980) to the conclusion that employment of the exponential function gave rise to very rapid convergence. Heyes & van Swol (1981) carried out an explicit comparison among several charge functions including the Gaussian and exponential, again for a simple cubic lattice. According to the results presented in their Table III, the Gaussian function denoted by their index $s=2$ converges faster than the exponential, $s=3$. However, the exponential-based potential initially obtains values closer to the final ones.

The choice of σ may have significant consequences on the rapidity of convergence of the potential sums, especially for larger or more complicated structures. For that reason a comparative study has been undertaken of the Gaussian and exponential functions which can be incorporated in the Ewald method. Their effect on the convergence of the potentials is investigated in terms of η using more complicated structures, partly based on non-orthogonal systems. The structures investigated here are: sodium chloride face (111); aragonite faces (001) and (112); phlogopite face (001).

When crystal growth occurs from aqueous solutions the electric field plays a dominant role in the behaviour of the interface; water molecules, being dipoles, respond by aligning themselves with the maximum field. Further work along this line is in progress.

2. Outline of theoretical results

The reader is referred to the Appendix for a complete list of definitions of symbols used in this section.

In applying the Ewald method, the charge density at **R** due to all ions in the lattice is split into two parts (Tosi, 1964) by adding and subtracting a continuous spherically symmetric charge distribution:

$$\rho_1^{\mathrm{tot}}(\mathbf{R})=\sum_{\mathbf{t}}\sum_{j=1}^{N} q_j\sigma(|\mathbf{R}-\mathbf{R}_j+\mathbf{t}|,\eta),$$
$$\rho_2^{\mathrm{tot}}(\mathbf{R})=\sum_{\mathbf{t}}\sum_{j=1}^{N} q_j[\delta(\mathbf{R}-\mathbf{R}_j+\mathbf{t})-\sigma(|\mathbf{R}-\mathbf{R}_j+\mathbf{t}|,\eta)], \quad (1)$$

where **t** is any lattice translation. The $\mathbf{t}=0$ terms give the charge density due to the N ions in the unit cell. The densities $\rho_1^{\mathrm{tot}}(\mathbf{R})$ and $\rho_2^{\mathrm{tot}}(\mathbf{R})$ in (1) give rise to potential expressions $U_1(\mathbf{R},\eta)$ and $U_2(\mathbf{R},\eta)$ treated in the reciprocal and direct space, respectively. The total physical potential is the real part of $U(\mathbf{R})=U_1(\mathbf{R},\eta)+U_2(\mathbf{R},\eta)$, and the slice energy is

$$E_{\mathrm{sl}}=\tfrac{1}{2}\sum_{j=1}^{N} q_jU(\mathbf{R}_j)$$

(Hartman, 1958).

To begin with the reciprocal space, the Fourier coefficient of $\rho_1^{\mathrm{tot}}(\mathbf{R},\eta)$ is (Tosi, 1964)

$$\rho_{\mathbf{K}}=(1/V)\sum_{j=1}^{N} q_j\exp(i\mathbf{K}.\mathbf{R}_j)\Phi(K,\eta);$$
$$\Phi(K,\eta)=(4\pi/K)\int_0^{\infty} x\sigma(x,\eta)\sin(Kx)\,\mathrm{d}x. \quad (2)$$

With the Gaussian and exponential forms for σ one gets (Heyes, 1980; Heyes & van Swol, 1981)

$$\sigma_{\mathrm{G}}(x,\eta)=\pi^{-3/2}\eta^{-3}\exp[-(x/\eta)^2],$$
$$\sigma_{\mathrm{E}}(x,\eta)=(8\pi\eta^3)^{-1}\exp(-x/\eta), \quad (3)$$

$$\int\sigma(x,\eta)\,\mathrm{d}\mathbf{x}=4\pi\int_0^{\infty}\sigma(x,\eta)x^2\,\mathrm{d}x=1,$$

$$\Phi_{\mathrm{G}}(K,\eta)=\exp(-K^2\eta^2/4),$$
$$\Phi_{\mathrm{E}}(K,\eta)=\eta^{-4}/(\eta^{-2}+K^2)^2. \quad (4)$$

Applying the definition of Coulomb potential to the Fourier decomposition of the charge using (2) one gets

$$U_1(\mathbf{R},\eta)=\int_{\text{all space}}(|\mathbf{R}'-\mathbf{R}|)^{-1}\times\sum_{\mathbf{K}}\exp[-i\mathbf{K}.(\mathbf{R}'-\mathbf{R})]\rho_{\mathbf{K}}\,\mathrm{d}\mathbf{R}'$$
$$=(4\pi/V)\sum_{j=1}^{N} q_j\sum_{\mathbf{K}}\frac{\Phi(K,\eta)}{K^2}\times\exp[i\mathbf{K}.(\mathbf{R}_j-\mathbf{R})]\quad\text{for }\mathbf{R}\neq\mathbf{R}_j. \quad (5)$$

It follows from (2) that as $\mathbf{K}\to 0$, $\rho_{\mathbf{K}}\to\sum_j q_j/V=0$, which vanishes due to charge neutrality of the unit cell. Hence since $\rho_0=0$, the $\mathbf{K}=0$ term in (5) does not contribute.

When **R** coincides with an ion site anywhere in a layer defined by $\mathbf{R}_j+u\mathbf{a}+v\mathbf{b}$ (u, v integers) the following self-potential expression for q_j must be subtracted because (5) originates from all charges, including q_j (Heyes 1980, 1981):

$$\int_{\text{all space}}\frac{q_j\sigma(|\mathbf{R}'-(\mathbf{R}_j+u\mathbf{a}+v\mathbf{b})|,\eta)}{|\mathbf{R}'-(\mathbf{R}_j+u\mathbf{a}+v\mathbf{b})|}\,\mathrm{d}\mathbf{R}'$$
$$=4\pi q_j\int_0^{\infty} x\sigma(x,\eta)\,\mathrm{d}x. \quad (6)$$

The potential due to the desired lattice shape, which is a slice, is obtained by the following two-step transformation carried out originally by Hartman (1958) and several other authors since then. **K** is decomposed into components **k** and **k**′, respectively parallel and perpendicular to (001); the position vector **R** is similarly decomposed into components **r** and **z**. In

the resulting expression (Heyes & van Swol, 1981),

$$U_1(\mathbf{R},\eta)=\sum_{j=1}^{N} q_j \sum_{\lambda,\mu} \exp[i\mathbf{k}\cdot(\mathbf{r}_j-\mathbf{r})](4\pi/V) \times \sum_{\nu=-\infty}^{\infty} \frac{\Phi[(k^2+k'^2)^{1/2},\eta]}{k^2+k'^2} \times \exp[ik'(z_j-z)], \quad (7)$$

the step from the bulk lattice to a slice one unit cell thick is accomplished by letting the period $c\to\infty$, while keeping the ion positions $\mathbf{R}_j$ fixed. The discrete variable ν becomes continuous, with the result (Jackson, 1963)

$$\lim_{c\to\infty}(1/V)\sum_{\nu=-\infty}^{\infty}\cdots=\frac{1}{2\pi A}\int_{-\infty}^{\infty}\cdots \mathrm{d}k';$$

$$\mathrm{d}\nu=(V/2\pi A)\,\mathrm{d}k'.$$

Finally,

$$U_1(\mathbf{R},\eta)=(2/A)\sum_{j=1}^{N} q_j \sum_{\lambda,\mu=-\infty}^{\infty} \exp[i\mathbf{k}\cdot(\mathbf{r}_j-\mathbf{r})] \times\psi(k,z_j-z,\eta) - \sum_{i=1}^{N} q_i \sum_{u,v=-\infty}^{\infty} U_0(\eta)\delta_{\mathbf{R},\mathbf{R}_i+u\mathbf{a}+v\mathbf{b}} \quad (8a)$$

where

$$\psi(k,z_j-z,\eta)=\int_{-\infty}^{\infty}\frac{\Phi[(k^2+k'^2)^{1/2},\eta]}{k^2+k'^2}\times\exp[ik'(z_j-z)]\,\mathrm{d}k',$$

and

$$U_0(\eta)=4\pi\int_0^{\infty} x\sigma(x,\eta)\,\mathrm{d}x. \quad (8b)$$

Further,

$$\psi_G(k,z_j-z,\eta)=(\pi/2k)[\exp(k|z_j-z|)\operatorname{erfc}(k\eta/2+|z_j-z|/\eta)+\exp(-k|z_j-z|)\operatorname{erfc}(k\eta/2-|z_j-z|/\eta)], \quad (9a)$$

$$\psi_E(k,z_j-z,\eta)=\pi\left\{\frac{\exp(-k|z_j-z|)}{k}-\frac{|z-z_j|\exp[-|z_j-z|(k^2+\eta^{-2})^{1/2}]}{2(k^2+\eta^{-2})\eta^2}-\frac{\exp[-|z_j-z|(k^2+\eta^{-2})^{1/2}](2k^2+3\eta^{-2})}{2(k^2+\eta^{-2})^{3/2}}\right\}, \quad (9b)$$

$$U_0^G(\eta)=2/\pi^{1/2}\eta,\quad U_0^E(\eta)=2/\eta, \quad (9c)$$

and in (9a) use has been made of

$$1/x^2=\int_0^{\infty}\exp(-x^2t)\,\mathrm{d}t.$$

The $\lambda=\mu=0$ term of (8a) is evaluated by taking the limit of (9a) and (9b) as $\mathbf{k}\to 0$ or reintegrating with the integrand at $\mathbf{k}=0$, ignoring divergent terms if they are multiplied by the total charge in the unit cell.

$$\psi_G(k=0,z_j-z,\eta)=-\pi|z_j-z|\operatorname{erf}(|z_j-z|/\eta)-\pi^{1/2}\eta\exp(-|z_j-z|^2/\eta^2), \quad (10)$$

$$\psi_E(k=0,z_j-z,\eta)=-\tfrac{1}{2}\pi[|z_j-z|+\exp(-|z_j-z|/\eta)(|z_j-z|+3\eta)].$$

Now consider a different slice, translated by $[00m]$ with respect to the slice treated thus far, where m is a positive or negative integer. Slice m contains ions located at $\mathbf{R}_j+m\mathbf{c}$ and is identical to the original slice when $m=0$. The potential originating from slice m is given by (8) when $\mathbf{R}_j$ is replaced by $\mathbf{R}_j+m\mathbf{c}$. This has consequences for the expressions z_j-z and $\mathbf{k}\cdot(\mathbf{r}_j-\mathbf{r})$, considering that the newly introduced displacement $m\mathbf{c}$ has distance $m\mathbf{c}\cdot\hat{\mathbf{n}}=mV/A$ from the (001) face and component $m[\mathbf{c}-(V/A)\hat{\mathbf{n}}]$ in that face. Thus $z_j-z\to z_j-z+mV/A$ and $\mathbf{k}\cdot(\mathbf{r}_j-\mathbf{r})\to\mathbf{k}\cdot(\mathbf{r}_j-\mathbf{r}+m\mathbf{c})$ in (8) and (9). Finally, the total potential of a collection of such slices, not necessarily a set of adjacent slices, is

$$U_1^{\mathrm{tot}}(\mathbf{R},\eta)=(2/A)\sum_{j=1}^{N} q_j \sum_{\substack{\lambda,\mu=-\infty\\ \lambda\neq 0\text{ or }\\ \mu\neq 0}}^{\infty}\sum_m \exp[i\mathbf{k}\cdot(\mathbf{r}_j-\mathbf{r})] \times\exp(im\mathbf{k}\cdot\mathbf{c})\psi(k,z_j-z+mV/A,\eta) + (2/A)\sum_{j=1}^{N} q_j\sum_m\psi(0,z_j-z+mV/A,\eta) - \sum_{j=1}^{N} q_j\sum_{\lambda,\mu=-\infty}^{\infty}\sum_m U_0(\eta)\delta_{\mathbf{R},\mathbf{R}_j+\lambda\mathbf{a}+\mu\mathbf{b}+m\mathbf{c}}$$

($\delta_{\mathbf{x},\mathbf{y}}=1$ if $\mathbf{x}=\mathbf{y}$, otherwise 0). (11)

Equation (11) is in slight disagreement with equations (20)-(22) of Heyes & van Swol (1981) where the factor $\exp(im\mathbf{k}\cdot\mathbf{c})$ does not appear. Only in the case of non-orthogonal unit cells does this factor have a value different from 1. This explains why Heyes & van Swol did not detect the error since they applied their formulas to orthogonal unit cells only.

Continuing with the potential contribution in the direct space, we find that the second charge density

of (1), characterized by slices $[00m]$,

$$\rho_2^{\text{tot}}(\mathbf{R}) = \sum_{j=1}^{N} q_j \sum_{\lambda,\mu=-\infty}^{\infty} \sum_m q_j[\delta(\mathbf{d}^j_{\lambda\mu m}) - \sigma(d^j_{\lambda\mu m}, \eta)], \tag{12}$$

leads to the potential

$$U_2(\mathbf{R}, \eta) = \sum_{j=1}^{N} q_j \sum_{\lambda,\mu=-\infty}^{\infty} \sum_m{}' [(d^j_{\lambda\mu m})^{-1} + I(d^j_{\lambda\mu m})] \tag{13a}$$

and the prime means that self-potential terms for which $\mathbf{R} = \mathbf{R}_j + \lambda\mathbf{a} + \mu\mathbf{b} + m\mathbf{c}$ are excluded from the summation. The integral

$$I(\mathbf{R}) = \int_{\text{all space}} \frac{-\sigma(x, \eta)}{|\mathbf{d}^j_{\lambda\mu m} - \mathbf{x}|} \, \mathrm{d}\mathbf{x}$$

arising from the σ function of (12) becomes

$$I(d^j_{\lambda\mu m}) = -2\pi[(1/d^j_{\lambda\mu m}) \int_0^{d^j_{\lambda\mu m}} x^2\sigma(x, \eta)\, \mathrm{d}x + \int_{d^j_{\lambda\mu m}}^{\infty} x\sigma(x, \eta)\, \mathrm{d}x] \tag{13b}$$

and further integration using σ_G and σ_E in (3) results in (*cf.* Heyes, 1980; Heyes & van Swol, 1981)

$$I_G(d^j_{\lambda\mu m}) = -(1/d^j_{\lambda\mu m}) \operatorname{erf}(d^j_{\lambda\mu m}/\eta);$$

$$I_E(d^j_{\lambda\mu m}) = \exp(-d^j_{\lambda\mu m}/\eta) \times (1/2\eta + 1/d^j_{\lambda\mu m}) - 1/d^j_{\lambda\mu m}. \tag{13c}$$

The electric field vector $\mathbf{E}$ is fully described by its projections on $\mathbf{a}$, $\mathbf{b}$, $\mathbf{c}$ (see also Heyes, 1981):

$$\mathbf{E}\cdot\mathbf{a}/a = (-4\pi/Aa) \sum_{j=1}^{N} q_j \times \sum_{\substack{\lambda,\mu=-\infty \\ \lambda\neq 0 \text{ or } \\ \mu\neq 0}}^{\infty} \sum_m \sin \mathbf{k}\cdot(\mathbf{r}_j - \mathbf{r} + m\mathbf{c}) \times \psi(k, z_j - z + mV/A, \eta) - \sum_{j=1}^{N} q_j \sum_{\lambda,\mu=-\infty}^{\infty} \sum_m{}' (Q_a/d^j_{\lambda\mu m}) \times [-(d^j_{\lambda\mu m})^{-2} + I'(d^j_{\lambda\mu m})],$$

$$\mathbf{E}\cdot\mathbf{b}/b = (-4\pi/Ab) \sum_{j=1}^{N} q_j \times \sum_{\substack{\lambda,\mu=-\infty \\ \lambda\neq 0 \text{ or } \\ \mu\neq 0}}^{\infty} \sum_m \sin \mathbf{k}\cdot(\mathbf{r}_j - \mathbf{r} + m\mathbf{c}) \times \psi(k, z_j - z + mV/A, \eta) - \sum_{j=1}^{N} q_j \sum_{\lambda,\mu=-\infty}^{\infty} \sum_m{}' (Q_b/d^j_{\lambda\mu m}) \times [-(d^j_{\lambda\mu m})^{-2} + I'(d^j_{\lambda\mu m})],$$

$$\mathbf{E}\cdot\mathbf{c}/c = (2V/A^2c) \sum_{j=1}^{N} q_j \times \sum_{\substack{\lambda,\mu=-\infty \\ \lambda\neq 0 \text{ or } \\ \mu\neq 0}}^{\infty} \sum_m [\cos \mathbf{k}\cdot(\mathbf{r}_j - \mathbf{r} + m\mathbf{c}) \times \psi'(k, z_j - z + mV/A, \eta) - (A/V)\mathbf{k}\cdot\mathbf{c} \sin \mathbf{k}\cdot(\mathbf{r}_j - \mathbf{r} + m\mathbf{c}) \times \psi(k, z_j - z + mV/A, \eta)] + (2V/A^2c) \sum_{j=1}^{N} q_j \sum_m \psi'(0, z_j - z + mV/A, \eta) - \sum_{j=1}^{N} q_j \sum_{\lambda,\mu=-\infty}^{\infty} \sum_m{}' (Q_c/d^j_{\lambda\mu m}) \times [-(d^j_{\lambda\mu m})^{-2} + I'(d^j_{\lambda\mu m})],$$

$$\psi'_G(k, y, \eta) = (\text{sign } y)(\pi/2) \times [\exp(k|y|) \operatorname{erfc}(k\eta/2 + |y|/\eta) - \exp(-k|y|) \operatorname{erfc}(k\eta/2 - |y|/\eta)],$$

$$\psi'_E(k, y, \eta) = (\text{sign } y)\pi\{-\exp(-k|y|) + \exp[-(k^2 + \eta^{-2})^{1/2}|y|] \times [1 + |y|/2(k^2 + \eta^{-2})^{1/2}\eta^2]\},$$

$$\psi'_G(0, y, \eta) = -\pi \operatorname{erf}(y/\eta),$$

$$\psi'_E(0, y, \eta) = -\pi (\text{sign } y) \times [1 - \exp(|y|/\eta)(1 + |y|/2\eta)],$$

with $y = (z_j - z + mV/A)$,

$$I'_G(y) = (1/y^2) \operatorname{erf}(y/\eta) - (2/\pi^{1/2})(1/\eta y) \exp(-y^2/\eta^2),$$

$$I'_E(y) = -\exp(-y/\eta)(1/2\eta^2 + 1/y\eta + 1/y^2),$$

with $y = d^j_{\lambda\mu m}$,

$$Q_a = (R_a - R^j_a - \lambda)a + (R_b - R^j_b - \mu)b \cos\gamma + (R_c - R^j_c - m)c \cos\beta,$$

$$Q_b = (R_b - R^j_b - \mu)b + (R_a - R^j_a - \lambda)a \cos\gamma + (R_c - R^j_c - m)c \cos\alpha,$$

$$Q_c = (R_c - R^j_c - m)c + (R_a - R^j_a - \lambda)a \cos\beta + (R_b - R^j_b - \mu)b \cos\alpha.$$

3. Computation

The APL program *SURFPOT* computes lamina potentials, energies and field vectors at arbitrary points with respect to a general structure. The choice between Gaussian or exponential form for σ and of a value for η is made by the user. The input data also include unit-cell parameters and ion coordinates

and charges. A suitable transformation matrix with determinant 1 may be optionally introduced to attain any required lamina orientation $(hkl) \neq (001)$. The point coordinates at which potential and field are to be evaluated are specified in the transformed system in one of three ways: (1) a set of ion sites (points that form part of the lattice); (2) a set of arbitrary points; (3) a sequence of grids parallel to (hkl) generated by two steps along the new $\mathbf{a}'$ and $\mathbf{b}'$ axes, and one step along the new $\mathbf{c}'$ axis. Apart from the above input, the user indicates values of m corresponding to slices from which the potential originates, *e.g.* $m = -2$ implies a slice removed from the zero slice by $-2\mathbf{c}'$. Although the potential of each individual slice converges, the potential of a semi-infinite lattice, approximated by a sequence of slices using *e.g.* $m = 0, -1, -2, \ldots$ will not converge, unless the component of the dipole moment of the unit cell perpendicular to (hkl) vanishes. For a slice of an F (*i.e.* flat) face several different ionic configurations may be possible, corresponding to different slice boundaries (Strom, 1985). It is essential to have a mechanism available for selecting specific, usually nonpolar, F configurations to represent an F slice. This is done by optionally assigning lattice translations to the individual ions in the unit cell, as will be illustrated by the examples of § 4, where all occurring slice configurations have been chosen nonpolar.

The terms in the double potential sums are evaluated in successive concentric ring-shaped regions defined by the radii $D_0 < D_1 < D_2 \ldots$ where $D_0 = 0$ and the step $D_n - D_{n-1}$ is internally determined and kept constant. Thus the contribution of the nth ring is obtained by including those (λ, μ) terms for which

$$D_{n-1} < (\lambda^2 a'^2 + \mu^2 b'^2 - 2\lambda\mu a'b' \cos\gamma')^{1/2} \leq D_n$$

in the case of U_1, and

$$D_{n-1} < (\lambda^2 a'^2 + \mu^2 b'^2 + 2\lambda\mu a'b' \cos\gamma)^{1/2} \leq D_n$$

in the case of U_2. The convergence distance D for the case under consideration is that D_N for which the Nth-ring contribution is below a small value. The U_1 and U_2 summations are carried out independently.

Of the functions occurring in § 2 only the error function is not available as primitive. For it the following polynomial approximation is chosen (Abramowitz & Stegun, 1965) for $0 \leq x$, and the symmetry property $\mathrm{erf}(x) = -\mathrm{erf}(-x)$ is employed for $x < 0$:

$$\mathrm{erf}\, x = 1 - (a_1 t + a_2 t^2 + a_3 t^3 + a_4 t^4 + a_5 t^5) \times \exp(-x^2) + \varepsilon(x),$$

$$t = 1/(1+px), \qquad |\varepsilon(x)| \leq 1{\cdot}5 \times 10^{-7},$$

$$p = 0{\cdot}327\,591\,1, \qquad a_1 = 0{\cdot}254\,829\,592,$$

$$a_2 = -0{\cdot}284\,496\,736, \qquad a_3 = 1{\cdot}421\,413\,741,$$

$$a_4 = -1{\cdot}453\,152\,027 \qquad a_5 = 1{\cdot}061\,405\,429.$$

4. Application

In the following examples the surface structure is assumed to be not relaxed and the slice configurations are nonpolar.

The NaCl unit-cell parameters are $a = b = c = 5{\cdot}6398$ Å, $\alpha = \beta = \gamma = 90°$. The choice of new axes $\mathbf{a}' = \mathbf{b} - \mathbf{a}$ and $\mathbf{b}' = \mathbf{c} - \mathbf{b}$ results in $(001)' = (111)$, where the primed indices refer to the transformed system. The simplest choice for $\mathbf{c}'$ leaving the unit-cell volume invariant is $\mathbf{c}' = \mathbf{c}$. Because a (111) surface bounded by a complete layer of either Na^+ or Cl^- ions is unstable, the surface structure has to be changed into an ordered puckered one, of which the outermost layer contains 1/4 and the second layer 3/4 of all available ions, as shown in Fig. 1. Thus the new unit cell has no dipole moment. Table 1 shows the resulting transformed cell parameters, the ion positions and the potentials at the ion sites due to slices $m = 0$, -1 and -2. The slice energy E_{sl} amounts to $-1{\cdot}95847\ e^2\ Å^{-1}$ per unit-cell content and the sum of the interaction energies with the 0 slice corresponds to $E_{att} = -0{\cdot}51350\ e^2\ Å^{-1}$. The total energy $E_{sl} + E_{att} = E_{cr} = -2{\cdot}47197\ e^2\ Å^{-1}$ per unit-cell content corresponds to the Coulomb part of the lattice energy. The value should be $-8\alpha/a$, where α is the Madelung

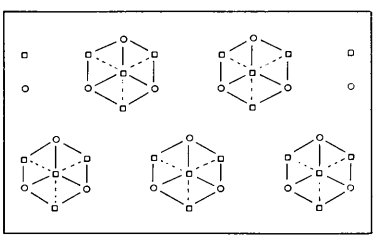

(*a*)

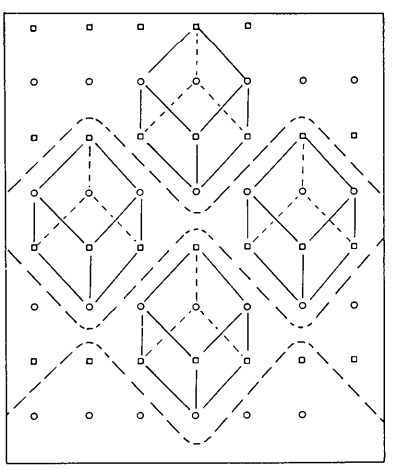

(*b*)

Fig. 1. Original NaCl unit cell in projection (*a*) onto plane (111), and (*b*) parallel to $[\bar{1}2\bar{1}]$ showing the slice configuration, bounded by the wavy broken lines, chosen for the (111) face. Squares: Na; circles: Cl.

Table 1. *Ion positions and charges in transformed* NaCl *unit cell with parameters* $a' = b' = 7{\cdot}9758$, $c' = 5{\cdot}6398$ Å, $\alpha' = 45$, $\beta' = 90$, $\gamma' = 120°$

Potentials at ion sites of (111) slices and energies.

Ion		x'	y'	z'	q	Potential (e Å^{-1}) Slice 0	Slice −1	Slice −2	Total
Cl(1)		0	0	0	−1	0·55145	0·13944	−0·08786	0·60303
Na(1)	$\bar{1}\,\bar{1}\,0$	−1/2	−1/2	1/2	1	−0·46900	−0·13549	0·00157	−0·60292
Na(2)	$\bar{1}\,0\,0$	−1/2	0	1/2	1	−0·46900	−0·13549	0·00157	−0·60292
Na(3)		0	0	1/2	1	−0·46900	−0·13549	0·00157	−0·60292
Cl(2)	$\bar{1}\,0\,1$	−1/2	0	1	−1	0·46900	0·01984	−0·00267	0·48617
Cl(3)	$\bar{1}\,\bar{1}\,1$	−1	−1/2	1	−1	0·46900	0·01984	−0·00267	0·48617
Cl(4)	$\bar{1}\,\bar{1}\,1$	−1/2	−1/2	1	−1	0·46900	0·01984	−0·00267	0·48617
Na(4)	$\bar{1}\,\bar{1}\,1$	−1	−1/2	3/2	1	−0·55145	−0·00735	−0·00131	−0·56012

Slice energy (e^2 Å^{-1}): −1·95847.
Interaction energy with slice 0 (e^2 Å^{-1}): −0·61279 (slice −1); 0·09929 (slice −2).
Total energy (e^2 Å^{-1}): $E_{cr} = -2{\cdot}47197$.

constant of the NaCl structure, 1·747558, leading to −2·47889. The discrepancy is due to neglect of slices −3, −4, *etc.* Fig. 2 illustrates the behaviour of the potential at the first ion site Cl(1), characteristic of the remaining sites. The contributions of the exponential- and Gaussian-based direct and reciprocal potential appear below the corresponding convergence distances D for $\eta = 3$ and 5 Å.

For the aragonite (001) and (112) faces the potential is computed at all ion sites, incorporating slices $m = 0, -1$ for (001), $m = 0, -1, -2, -3$ for slices (112), and using η values between 2 and 6 Å. For the (001) slice use is made of the original orthogonal unit cell. The slice boundaries are defined by the untranslated ions. Cell parameters, ion coordinates, potentials and energies are shown in Table 2. The choice of new axes $\mathbf{a}' = \mathbf{a} - \mathbf{b}$, $\mathbf{b}' = \mathbf{a} + \mathbf{b} - \mathbf{c}$ leads to $(001)' = (112)$,

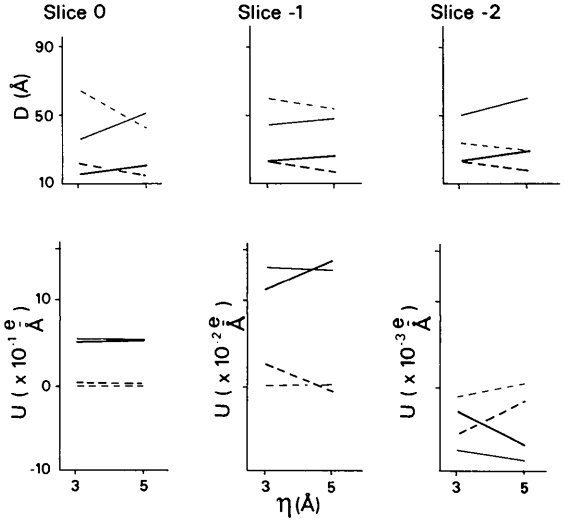

Fig. 2. Dependence on η of convergence radius and potential, both approximated by straight lines, of NaCl face (111) at the Cl(1) ion site, for slices 0, −1 and −2. Thick lines: Gaussian based; thin lines: exponential based; solid lines: direct-space contribution; dashed lines: reciprocal-space contribution.

and $\mathbf{c}' = \mathbf{a}$ is an acceptable possibility. The (112) slice boundaries are defined by introducing lattice translations to the ions, as shown in Table 3, along with the transformed cell parameters, potentials and energies. Slice configurations for both the (001) and (112) faces are shown in Heijnen's (1986) structure projection perpendicular to $[\bar{1}10]$ in Fig. 3. The Ca(1), O(1) and O(6) ion sites suffice to illustrate the behaviour of the potentials, shown in Figs. 4 and 5 below the convergence distance D. The values are in good agreement with those of Heijnen (1986) who obtained for the total energy −3112·3 kJ mol^{-1}, which corresponds to −12·915 e^2 Å^{-1} for the four molecules present in the unit cell, when the energy of the CO_3 group is taken into account (−0·98867 e^2 Å^{-1}). Heijnen's value for the slice energy of (112) then becomes −11·4998 e^2 Å^{-1}.

The cell parameters and ion positions used for the (001) slice of phlogopite are listed in Table 4. The surface potential and electric field components are computed at points of a grid with $x = 0, 0{\cdot}1, \ldots, 1{\cdot}0$ along the a axis, $y = 0, 0{\cdot}05, 0{\cdot}1, \ldots, 0{\cdot}5$ along the b axis, at levels parallel to (001) defined by $z = 0{\cdot}85$, $0{\cdot}9, \ldots, 1{\cdot}25$ along the c axis. Because of convergence efficiency considerations the Gaussian choice is used. The contribution of slice $m = -1$ is negligible compared with that of slice $m = 0$, hence the latter slice in the case of phlogopite approximates satisfactorily the semi-infinite lattice bounded by (001). Curves of constant potential U and electric field magnitude $|\mathbf{E}|$ are shown as contour plots for $z = 0{\cdot}85$ and 1·0 in Figs. 6 and 7, superimposed on a structure projection on (001), using the upper half of the unit cell.

Elaboration on the phlogopite results is beyond the scope of this paper because a study of phlogopite and in particular its interaction with water is now in progress.

5. Concluding remarks

The results obtained from the NaCl and aragonite cases show remarkable similarities. The convergence

Table 2. *Ion positions and charges in aragonite unit cell with parameters* $a = 4{\cdot}9614$, $b = 7{\cdot}9671$, $c = 5{\cdot}7404$ Å, $\alpha = \beta = \gamma = 90°$

Potentials at all ion sites and energy of (001).

Ion	x	y	z	q	Potential (e Å^{-1}) Slice 0	Slice −1	Total
Ca(1)	0·2500	0·4150	0·7597	2	−1·0048	0·0054	−0·9994
Ca(2)	0·7500	0·5850	0·2403	2	−1·0048	−0·0840	−1·0888
Ca(3)	0·7500	0·9150	0·7403	2	−1·0888	−0·0046	−1·09348
Ca(4)	0·2500	0·0850	0·2597	2	−1·0888	0·0091	−1·07978
C(1)	0·2500	0·7622	0·9138	1	−1·3518	−0·0049	−1·3567
C(2)	0·7500	0·2378	0·0862	1	−1·3518	0·1518	−1·2
C(3)	0·7500	0·2622	0·5862	1	−1·1763	0·0210	−1·1553
C(4)	0·2500	0·7378	0·4138	1	−1·1763	−0·0471	−1·2234
O(1)	0·2500	0·9225	0·9038	−1	0·8562	−0·0025	0·8537
O(2)	0·7500	0·0775	0·0962	−1	0·8562	0·1585	1·0147
O(3)	0·7500	0·4225	0·5962	−1	1·0243	0·0088	1·0331
O(4)	0·2500	0·5775	0·4038	−1	1·0243	−0·0198	1·0045
O(5)	0·4736	0·6810	0·9138	−1	0·8437	−0·0044	0·8393
O(6)	0·0264	0·8190	0·4138	−1	1·0586	−0·0406	1·018
O(7)	0·9736	0·3190	0·0862	−1	0·8437	0·1954	1·0391
O(8)	0·5264	0·1810	0·5862	−1	1·0586	0·0189	1·0775
O(9)	0·5264	0·3190	0·0862	−1	0·8437	0·1954	1·0391
O(10)	0·9736	0·1810	0·5862	−1	1·0586	0·0189	1·0775
O(11)	0·0264	0·6810	0·9138	−1	0·8437	−0·0044	0·8393
O(12)	0·4736	0·8190	0·4138	−1	1·0586	−0·0406	1·018

Slice energy (e^2 Å^{-1}): −12·40047.
Interaction energy with slice 0 (e^2 Å^{-1}): −0·5110 (slice −1).
Total energy (e^2 Å^{-1}): $E_{cr} = -12{\cdot}9115$.

Table 3. *Ion positions in aragonite transformed unit cell with parameters* $a' = 9{\cdot}38564$, $b' = 11{\cdot}00193$, $c' = 4{\cdot}9614$ Å, $\alpha' = 63{\cdot}195$, $\beta' = 58{\cdot}088$, $\gamma' = 112{\cdot}106°$

Potentials at all ion sites and energy of (112) slices. (Ionic charges as in Table 2.)

Ion		x'	y'	z'	Potential (e Å^{-1}) Slice 0	Slice −1	Slice −2	Slice −3	Total
Ca(1)	$\bar{1}00$	−1·1747	−0·7597	1·1844	−0·9534	−0·0362	−0·0366	0·0049	−1·0213
Ca(2)	$\bar{1}00$	−0·8253	−0·2403	0·8156	−0·9534	−0·1951	+0·0497	−0·0049	−1·1038
Ca(3)	$\bar{2}00$	−1·6553	−0·7403	1·1456	−0·9626	−0·0157	−0·0172	0·0075	−0·9880
Ca(4)		−0·3447	−0·2597	0·8544	−0·9626	−0·2408	0·0593	−0·0032	−1·1474
C(1)	$\bar{2}00$	−1·6760	−0·9138	0·8398	−1·6057	0·2440	−0·0083	−0·0055	−1·3755
C(2)		−0·3240	−0·0862	1·1602	−1·6057	0·0848	0·0011	−0·0063	−1·5260
C(3)	$\bar{1}00$	−0·8484	−0·5862	1·1846	−1·2131	−0·0738	−0·0048	0·0058	−1·2859
C(4)	$\bar{1}00$	−1·1516	−0·4138	0·8154	−1·2131	−0·0337	0·0249	0·0059	−1·2160
O(1)	$\bar{2}00$	−1·8263	−0·9038	0·9801	0·5656	0·2083	−0·0175	−0·0001	0·7564
O(2)		−0·1737	−0·0962	1·0199	0·5656	0·1549	0·0160	−0·0072	0·7293
O(3)	$\bar{1}00$	−1·0187	−0·5962	1·3649	1·0032	−0·0862	0·0016	0·0027	0·9213
O(4)	$\bar{1}00$	−0·9813	−0·4038	0·6351	1·0032	0·0120	−0·0140	0·0085	1·0098
O(5)	$\bar{2}00$	−1·5948	−0·9138	0·9822	0·6390	0·2110	−0·0161	−0·0037	0·8302
O(6)	$\bar{1}00$	−1·2328	−0·4138	0·6730	1·0272	−0·0115	0·0194	0·0118	1·0469
O(7)		−0·4052	−0·0862	1·4650	0·6538	0·0422	−0·0118	−0·0020	0·6821
O(8)	$\bar{1}00$	−0·7672	−0·5862	0·8798	0·9576	0·0629	−0·0381	0·0119	0·9944
O(9)		−0·4052	−0·0862	1·0178	0·6390	0·1174	0·0063	−0·0098	0·7529
O(10)	$\bar{1}00$	−0·7672	−0·5862	1·3270	1·0272	−0·1095	0·0092	0·0038	0·9307
O(11)	$\bar{2}00$	−1·5948	−0·9138	0·5350	0·6538	0·2673	0·0096	−0·0153	0·9153
O(12)	$\bar{1}00$	−1·2328	−0·4138	1·1202	0·9576	−0·0805	0·0351	0·0002	0·9124

Slice energy (e^2 Å^{-1}): −11·4974.
Interaction energy with slice 0 (e^2 Å^{-1}): −1·5427 (slice −1); 0·1236 (slice −2); 0·0075 (slice −3).
Total energy (e^2 Å^{-1}): $E_{cr} = -12{\cdot}909$.

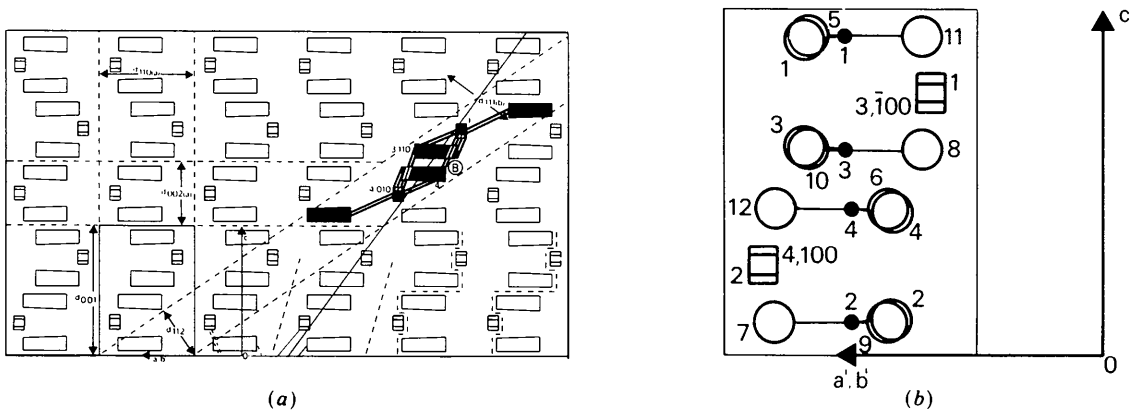

Fig. 3. (*a*) Heijnen's (1986) aragonite ($CaCO_3$) structure projection perpendicular to [$\bar{1}$10] with slices d_{001} and d_{112} indicated by dashed lines; rectangles: CO_3; squares: Ca. The squares partly overlap because they nearly coincide as seen in (*b*) which is a unit cell projected perpendicular to [$\bar{1}$10]. Small filled circles: C; large open circles: O. The area in black in (*a*) has a special significance not related to the present subject (the figure was copied from Heijnen's work).

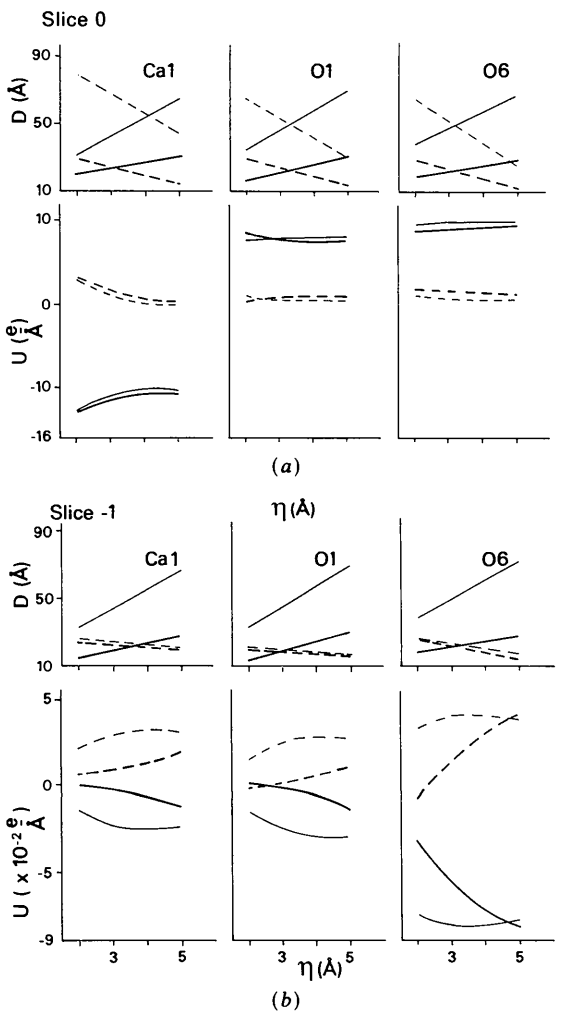

Fig. 4. Dependence on η of convergence radius approximated by a straight line, and potential approximated when possible by a smooth curve, of aragonite face (001) at ion sites Ca(1), O(1) and O(6). Line drawn according to Fig. 2. (*a*) Slice 0; (*b*) slice −1.

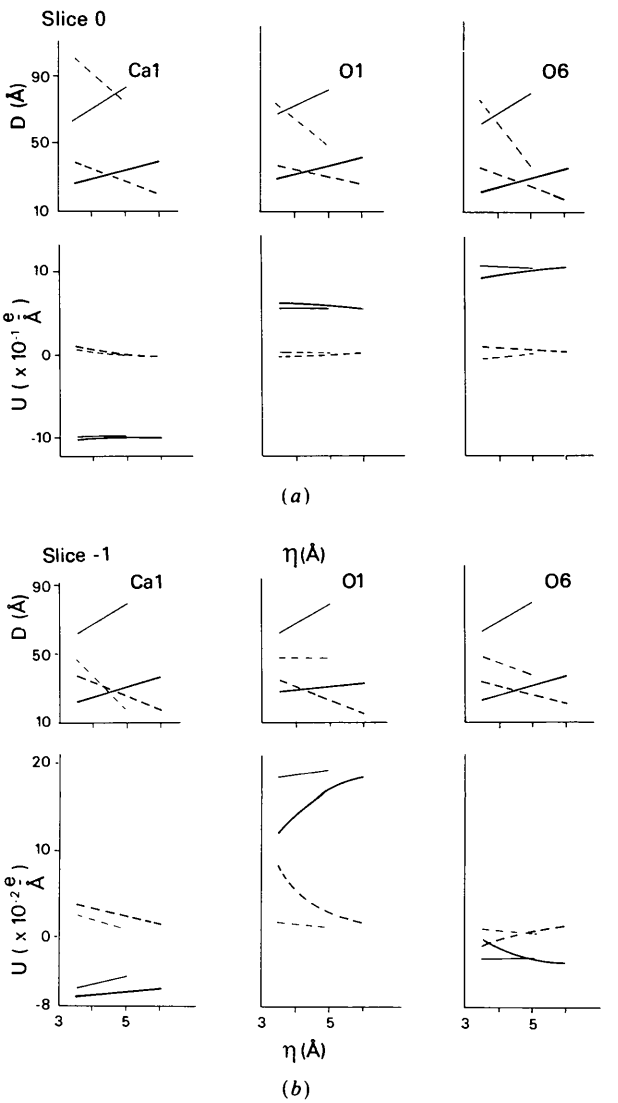

Fig. 5. Same as Fig. 4 for aragonite face (112).

distance required for the exponential choice is consistently and considerably larger than for the Gaussian. This effect is particularly pronounced in the $m = 0$ (112) slice of aragonite. Indeed there is not a single example in which the exponential function offers any advantage over the Gaussian or is even as satisfactory.

The Gaussian-based potential is more sensitive to the choice of η. The dominance of the direct contribution over the reciprocal one decreases as the distance between sampling point and slice increases, as expected.

We are grateful to Drs A. M. M. Schreurs for putting his program *CONTOUR* at our disposal and to Drs E. van der Voort for her assistance in running some test cases.

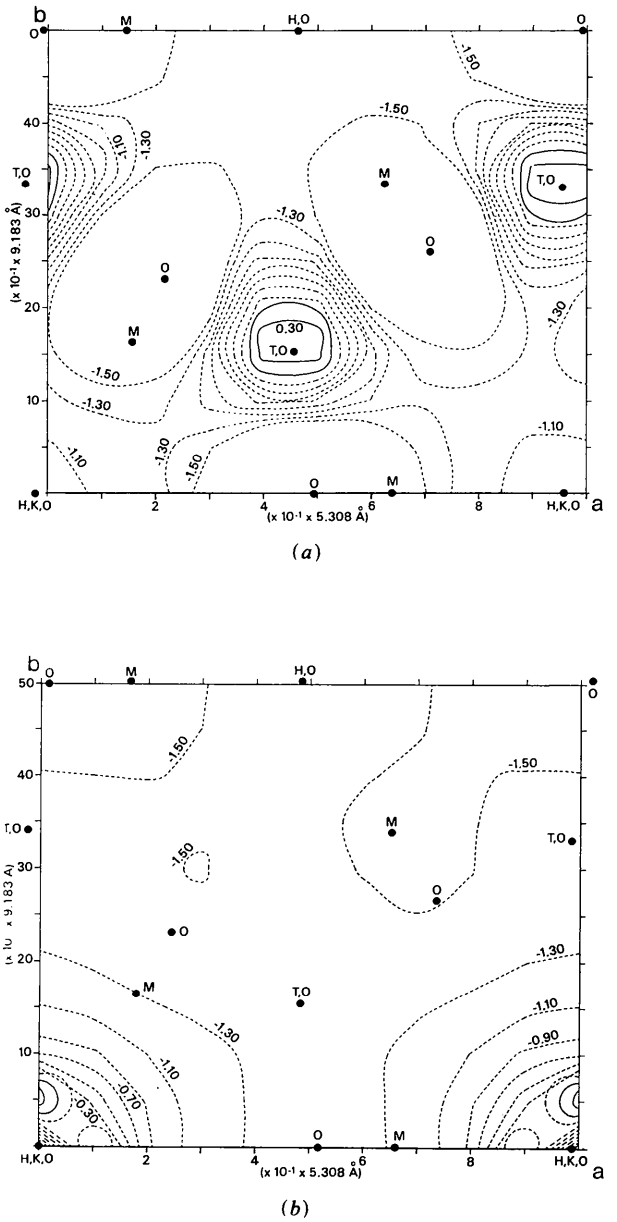

Fig. 6. Surface potential of phlogopite (Table 4), $KM_3T_4O_{10}(OH)_2$ with M = divalent cation such as Mg^{2+} and $T_4 = Si_3Al$, disordered, shown as contours (Schreurs, 1985), superimposed on a projection on the upper half of the unit cell on (001). (*a*) At height 0·85 along the *c* axis; (*b*) at height 1·0. Because of the low number of points, equipotential surfaces cross in (*b*).

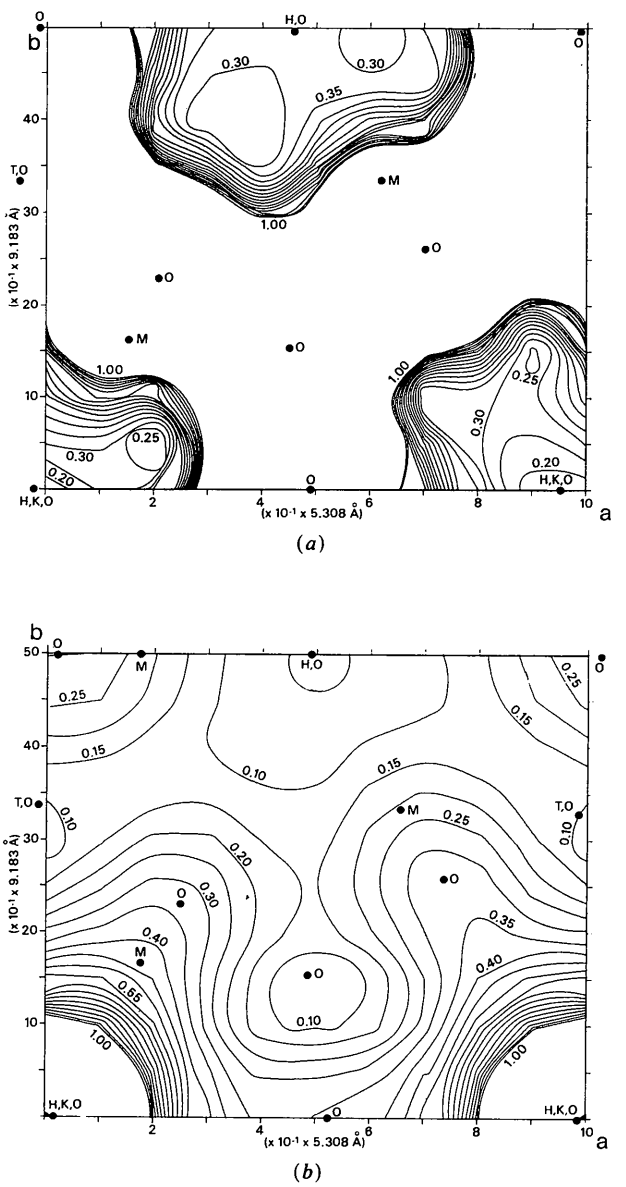

Fig. 7. Same as Fig. 6 for the electric field magnitude.

Table 4. *Ion positions and charges in phlogopite unit cell with parameters* $a = 5{\cdot}308$, $b = 9{\cdot}183$, $c = 10{\cdot}14$ Å, $\alpha = \gamma = 90$, $\beta = 100{\cdot}07°$, *used for the* $m = 0$ (001) *slice*

Ion	x	y	z	q	Ion	x	y	z	q
K(11), 001	0	0	1	1	O(13)	0·0274	0·5	0·1678	−2
K(12)	0·5	0·5	0	1	O(14)	0·9726	0·5	0·8322	−2
T(1)	0·4249	0·1663	0·7755	3·75	O(21)	0·1792	0·2347	0·8318	−2
T(2)	0·5751	0·8337	0·2245	3·75	O(22)	0·8208	0·7653	0·1682	−2
T(3)	0·5751	0·1663	0·2245	3·75	O(23)	0·8208	0·2347	0·1682	−2
T(4)	0·4249	0·8337	0·7755	3·75	O(24)	0·1792	0·7653	0·8318	−2
T(5)	0·9249	0·6663	0·7755	3·75	O(25)	0·6792	0·7347	0·8318	−2
T(6)	0·0751	0·3337	0·2245	3·75	O(26)	0·3208	0·2653	0·1682	−2
T(7)	0·0751	0·6663	0·2245	3·75	O(27)	0·3208	0·7347	0·1682	−2
T(8)	0·9249	0·3337	0·7755	3·75	O(28)	0·6792	0·2653	0·8318	−2
M(11)	0	0·1694	0·5	2	O(31)	0·3709	0·1661	0·6104	−2
M(12)	0·5	0·6694	0·5	2	O(32)	0·6291	0·8339	0·3896	−2
M(13)	0	0·8306	0·5	2	O(33)	0·6291	0·1661	0·3896	−2
M(14)	0·5	0·3306	0·5	2	O(34)	0·3709	0·8339	0·6104	−2
M(21)	0	0·5	0·5	2	O(35)	0·8709	0·6661	0·6104	−2
M(22)	0·5	0	0·5	2	O(36)	0·2191	0·3339	0·3896	−2
H(1)	0·0992	0	0·3015	1	O(37)	0·1291	0·6661	0·3896	−2
H(2)	0·9008	0	0·6985	1	O(38)	0·8709	0·3339	0·6104	−2
H(3)	0·5992	0·5	0·3015	1	O(41)	0·1327	0	0·4017	−2
H(4)	0·4008	0·5	0·6985	1	O(42)	0·8673	0	0·5983	−2
O(11)	0·5274	0	0·1678	−2	O(43)	0·6327	0·5	0·4017	−2
O(12)	0·4726	0	0·8322	−2	O(44)	0·3673	0·5	0·5983	−2

APPENDIX
List of symbols

$\mathbf{a}$, $\mathbf{b}$, $\mathbf{c}$, and $\mathbf{a}^*$, $\mathbf{b}^*$, $\mathbf{c}^*$	Direct- and reciprocal-lattice vectors
$\mathbf{a}^* = \mathbf{b}\times\mathbf{c}/V$ *etc.*	
α, β, γ	Lattice angles
$V = \mathbf{a}\,.\,\mathbf{b}\times\mathbf{c}$	Unit-cell volume
$A = \lvert\mathbf{a}\times\mathbf{b}\rvert$	Unit-cell area ∥ (001)
$\hat{\mathbf{n}} = \mathbf{c}^*/c^*$, with $c^* = A/V$	The (001) face normal
$\mathbf{K} = 2\pi(\lambda\mathbf{a}^* + \mu\mathbf{b}^* + \nu\mathbf{c}^*)$	Reciprocal-lattice translation
λ, μ, ν integers	
$\mathbf{k}' = 2\pi(\lambda\mathbf{a}^*\,.\,\hat{\mathbf{n}} + \mu\mathbf{b}^*\,.\,\hat{\mathbf{n}} + \nu c^*)\hat{\mathbf{n}}$	Component of $\mathbf{K}$ ⊥(001)
$\boldsymbol{k} = 2\pi\hat{\mathbf{n}}\times(\lambda\mathbf{a}^*\times\hat{\mathbf{n}} + \mu\mathbf{b}^*\times\hat{\mathbf{n}}) = (2\pi/A)(\lambda\mathbf{b}\times\hat{\mathbf{n}} + \mu\hat{\mathbf{n}}\times\mathbf{a})$	Component of $\mathbf{K}$ ∥(001)
$K = (k^2 + k'^2)^{1/2}$, $k = \lvert\mathbf{k}\rvert = (2\pi/A)(\lambda^2b^2 + \mu^2a^2 - 2\lambda\mu ab\cos\gamma)^{1/2}$,	
$\mathbf{k}\,.\,\mathbf{c} = -(2\pi c/\sin^2\gamma)[(\lambda/a)(\cos\alpha\cos\gamma - \cos\beta) + (\mu/b)(\cos\beta\cos\gamma - \cos\alpha)]$	
$\mathbf{R}_j = R_a^j\mathbf{a} + R_b^j\mathbf{b} + R_c^j\mathbf{c} = \mathbf{r}_j + \mathbf{z}_j$; $q_j, j = 1, \ldots, N$	Ion positions and charges
$\mathbf{R} = R_a\mathbf{a} + R_b\mathbf{b} + R_c\mathbf{c} = \mathbf{r} + \mathbf{z}$	Arbitrary position vector
$\mathbf{r}, \mathbf{r}_j$∥(001) and $\mathbf{z}, \mathbf{z}_j$⊥(001)	
$\mathbf{k}\,.\,(\mathbf{r}_j - \mathbf{r} + m\mathbf{c}) = 2\pi[\lambda(R_a^j - R_a) + \mu(R_b^j - R_b)] + (R_c^j - R_c + m)\mathbf{k}\,.\,\mathbf{c}$,	
$z_j - z + mV/A = (R_c^j - R_c + m)\,V/A$,	
$\mathbf{t} = \lambda\mathbf{a} + \mu\mathbf{b} + m\mathbf{c}$	Direct-lattice translation
λ, μ, m integers	m is slice index
$\mathbf{d}^j_{\lambda\mu m} = \mathbf{R} - \mathbf{R}_j - \lambda\mathbf{a} - \mu\mathbf{b} - m\mathbf{c}$, $d^j_{\lambda\mu m} = \lvert\mathbf{d}^j_{\lambda\mu m}\rvert$	
erf	Error function
erfc	Complementary error function

References

ABRAMOWITZ, M. & STEGUN, I. A. (1965). *Handbook of Mathematical Functions*, p. 229. New York: Dover.

EWALD, P. P. (1921). *Ann. Phys. (Leipzig)*, **64**, 253-287.

HARTMAN, P. (1958). *Acta Cryst.* **11**, 365-369.

HEIJNEN, W. M. M. (1986). *Neues Jahrb. Mineral. Abh.* **154**, 223-245.

HEYES, D. M. (1980). *J. Phys. Chem. Solids*, **41**, 281-293.

HEYES, D. M. (1981). *J. Chem. Phys.* **74**, 1924-1929.

HEYES, D. M. & VAN SWOL, F. (1981). *J. Chem. Phys.* **75**, 5051-5058.

JACKSON, J. D. (1963). *Classical Electrodynamics*, pp. 4, 8, 47. New York: John Wiley.

SCHREURS, A. M. M. (1985). *CONTOUR*. Unpublished Fortran program. Vakgroep Algemene Chemie, Rijksuniv. Utrecht, The Netherlands.

STROM, C. S. (1985). *Z. Kristallogr.* **172**, 11-24.

TOSI, M. (1964). *Solid State Physics*, Vol. 16, edited by F. SEITZ & D. TURNBULL, pp. 1-120. New York: Academic Press.